The Zoo of emission lines in the spectrum of Cir X–1 observed by XMM-Newton

R. Iaria, A. D'Ai', T. Di Salvo, G. Lavagetto and N. R. Robba

DSFA-Universita' degli Studi di Palermo

Abstract. We present the preliminary analysis of a 10 ks XMM-Newton EPIC/pn observation of Cir X–1 immediately after the zero phase. The continuum emission is modeled using a blackbody component partially absorbed by neutral matter probably located around the binary system. We detect a forest of emission lines associated to highly ionized ions.

Keywords: Photoionization of atoms and ions, Atomic processes and interactions, Atomic and molecular data, spectra, and spectral parameters.
PACS: 32.80.Fb, 95.30.Dr, 95.30.Ky

INTRODUCTION

Cir X–1 is a peculiar low-mass X-ray binary (LMXB). The detection of type I X-ray bursts (Tennant et al. 1986a, 1986b) indicates that the compact object is a neutron star. The canonical scenario accepted for Cir X-1 argues that the source has a companion star of $3-5$ $M_{\odot}$ (probably a subgiant; see Johnston et al. 1999), an orbital period of 16.6 days, deduced from the radio and X-ray light curve of the source, and an eccentric orbit with $e \simeq 0.7-0.9$ (Murdin et al. 1980; Tauris et al. 1999).

Using BeppoSAX data, Iaria et al. (2001a) analyzed the 0.1–100 keV spectrum of Cir X–1 at phases 0.11–0.16. They detected a strong absorption edge at $8.4-8.7$ keV, produced by highly ionized iron. Iaria et al. (2001b), using ASCA data, studied the energy spectrum of Cir X–1, along its period, distinguishing three different X-ray states of the source as a function of its phase. At the phases near phase zero, the hydrogen column derived from the edge was 10^{24} cm^{-2}; at larger values of the phase the hydrogen column decreased; the absorption edge (from ionized iron) was no longer detected at phases from 0.78 to 1, while at these phases a partial covering component was required with an equivalent hydrogen column of 10^{24} cm^{-2}.

Recently two relevant detections interested Cir X–1: 1) the detection of P-Cygni profiles at phase 0.99 (Brandt & Shulz, 2000; Shulz & Brandt, 2002). The presence of these features in the spectrum of Cir X–1 indicates that an outflow of matter with a velocity of 2000 km/s is present. Assuming that the source is seen nearly edge-on the authors describe a scenario in which the outflow of matter is produced in the outer region of the accretion disc following the prescription of thermally driven wind reported by Begelman et al. (1983); 2) the radio detection of an ultrarelativistic outflows similar to those produced by active galactic nuclei (Fender et al. 2004) with a superluminar motion of the jet with an apparent velocity of $15c$. The detection of the superluminal motion in the jet of Cir X–1 implies that θ, the angle between the line of sight and the direction of the jet, should be less than 5°. Since the jet should have a direction almost

CP924, *The Multicolored Landscape of Compact Objects and their Explosive Origins - Cefalù 2006,*
edited by T. Di Salvo, L. A. Antonelli, G. L. Israel, L. Piersanti, A. Tornambè, L. Burderi, F. Fiore, G. Matt, and M. T. Menna

perpendicular to the accretion disk it implies that Cir X–1 is seen face-on.

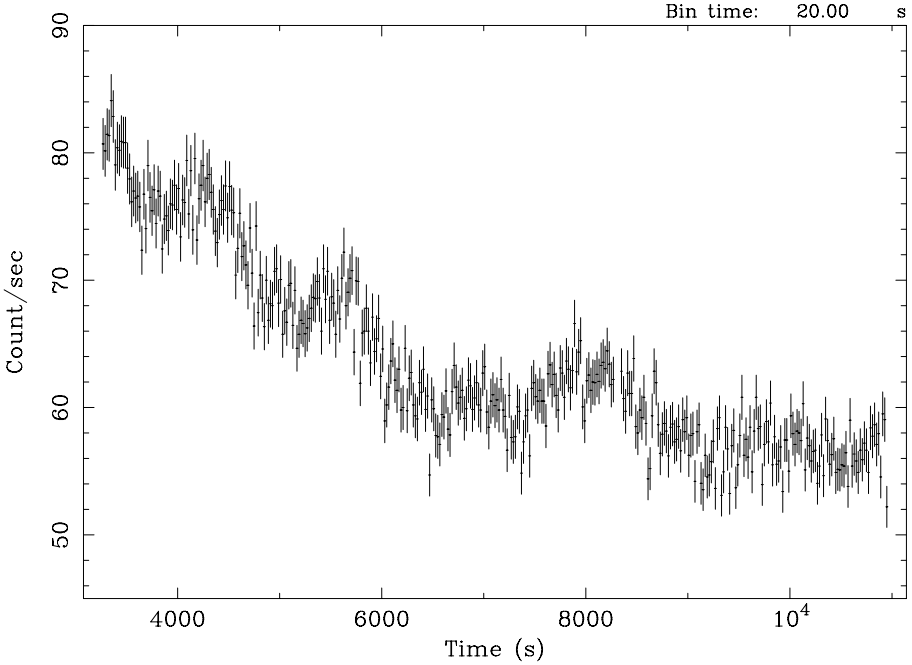

FIGURE 1. EPIC/pn lightcurve of Cir X–1, the bin time is 20 s.

OBSERVATION AND SPECTRAL ANALYSIS

The XMM-Newton Observatory (Jansen et al. 2001) includes three 1500 cm^2 X-ray telescopes each with an European Photon Imaging Camera (EPIC) at the focus. Two of the EPIC imaging spectrometers use MOS CCDs (Turner et al. 2001) and one uses pn CCDs (Struder et al. 2001). Reflection Grating Spectrometers (RGS, Den Herder et al. 2001) are located behind two of the telescopes. We analyze the 10 ks observation of Cir X–1 taken from the XMM public archive (Obsid 94520201). During the observation only EPIC-pn, operating in Timing mode, and RGS were active. Since we have interest to study the Fe-K region we analyze only the pn data reducing them using the Science Analysis Software (SAS) version 7.0.0 and calibration files released on 16 May 2006. In pn Timing mode, only one CCD chip is used and the data from that chip are collapsed into a one-dimensional row to be read out at high speed. This allows a time resolution of 30 μs, and photon pile-up occurs only for count rates higher than 1500 s^{-1}, much higher than the value observed during our observation (see Fig. 1). Using the ephemeris of Stewart et al. (1993) we find that the phase interval of the observation is 0.011–0.017, immediately after the phase-zero. We extract the energy spectrum in the energy band 0.7–10 keV. The continuum emission is fitted using a blackbody model absorbed by interstellar neutral matter and partially by neutral matter around the system. The

TABLE 1. Continuum emission and absorption edges

Parameters*		**Parameters**	
N_H ($\times 10^{22}$ cm^{-2})	1.22 ± 0.08	$E_{Si\ I}$ (keV)	1.871 (fixed)
$N_{H_{pc}}$ ($\times 10^{22}$ cm^{-2})	98^{+5}_{-9}	$\tau_{Si\ I}$	$0.46^{+0.04}_{-0.03}$
f_{pc}	0.75 ± 0.03	$E_{Si\ XIV}$ (keV)	2.673 (fixed)
kT_{BB} (keV)	1.21 ± 0.02	$\tau_{Si\ XIV}$	$0.11^{+0.03}_{-0.04}$
N_{BB}	0.025 ± 0.001	$E_{Ca\ I}$ (keV)	4.069 (fixed)
$E_{O\ VIII}$ (keV)	0.871 (fixed)	$\tau_{Ca\ I}$	< 0.03
$\tau_{O\ VIII}$	$0.72^{+0.33}_{-0.38}$	$E_{Fe\ XXV}$ (keV)	8.828 (fixed)
$E_{Ne\ IX}$ (keV)	1.196 (fixed)	$\tau_{Fe\ XXV}$	< 0.07
$\tau_{Ne\ IX}$	$0.41^{+0.14}_{-0.12}$	$E_{Fe\ XXVI}$ (keV)	$9.6^{+0.5}_{-0.2}$
$E_{Ne\ X}$ (keV)	1.362 (fixed)	$\tau_{Fe\ XXVI}$	0.09 ± 0.08
$\tau_{Ne\ X}$	$0.12^{+0.06}_{-0.07}$		

* Uncertainties are at 90% confidence level for a single parameter; upper limits are at 95% confidence level. The threshold energy of the absorption edges are taken from Verner et al., 1996a

TABLE 2. Emission and absorption lines

Ion*	**Measured E keV**	**Predicted E† keV**	**Transition**	**Width eV**	**Flux****
Ne X	$1.01^{+0.03}_{-0.04}$	1.0218	1s-2p	10 (fixed)	$2.8^{+1.5}_{-1.8}$
Mg XI	1.3523 (fixed)	1.3523	$1s^2$-1s2p	10 (fixed)	$2.7^{+0.7}_{-0.8}$
Mg XII	1.4723 (fixed)	1.4723	1s-2p	10 (fixed)	2.6 ± 0.6
Si XIV	$1.979^{+0.005}_{-0.004}$	2.0054	1s-2p	40 ± 5	$9.7^{+1.4}_{-1.0}$
S XV	$2.42^{+0.03}_{-0.02}$	2.4607	$1s^2$-1s2p	50^{+40}_{-50}	$2.5^{+1.6}_{-0.7}$
S XVI	2.63 ± 0.01	2.6216	1s-2p	40^{+20}_{-30}	$3.9^{+0.8}_{-0.7}$
Ar XVII	$3.11^{+0.02}_{-0.01}$	3.1398	$1s^2$-1s2p	< 20	1.2 ± 0.3
Ar XVIII	3.314 ± 0.014	3.3213	1s-2p	< 50	1.3 ± 0.3
Ca XIX(r)	3.9 ± 0.2	3.9023	$1s^2$-1s2p	< 60	$0.8^{+0.3}_{-0.2}$
Ca XX	$4.10^{+0.01}_{-0.03}$	4.1049	1s-2p	< 70	$0.8^{+0.3}_{-0.2}$
Fe I	6.39 ± 0.01	6.400	–	< 50	1.4 ± 0.2
Fe XXV(i)	6.657 ± 0.003	6.6749	$1s^2$-1s2p	40^{+7}_{-8}	4.6 ± 0.2
Fe XXVI	6.96 ± 0.01	6.9660	1s-2p	< 30	1.1 ± 0.1
Ni XXVII(r)	7.80 ± 0.01	7.7958	$1s^2$-1s2p	10 (fixed)	0.8 ± 0.1
Ni XXVIII	$8.16^{+0.04}_{-0.07}$	8.0871	1s-2p	10 (fixed)	0.3 ± 0.1
Fe XXVI	$8.34^{+0.08}_{-0.09}$	8.2499	1s-3p	10 (fixed)	0.2 ± 0.1
Fe XXVI	8.67 ± 0.03	8.6997	1s-4p	10 (fixed)	0.29 ± 0.07
Fe XXVI	8.91 ± 0.04	8.9079	1s-5p	10 (fixed)	0.27 ± 0.09
Line$_1$‡	5.6 ± 0.1	–	–	< 80	$0.2^{+0.8}_{-0.1}$
Line$_2$§	$5.85^{+0.30}_{-0.07}$	–	–	< 80	-0.2 ± 0.1

* Uncertainties are at 90% confidence level for a single parameter; upper limits are at 95% confidence level.

† The values are taken from Verner et al., 1996b

** ($\times 10^{-3}$ photons cm^{-2} s^{-1})

‡ Emission line not identified

§ Absorption line not identified

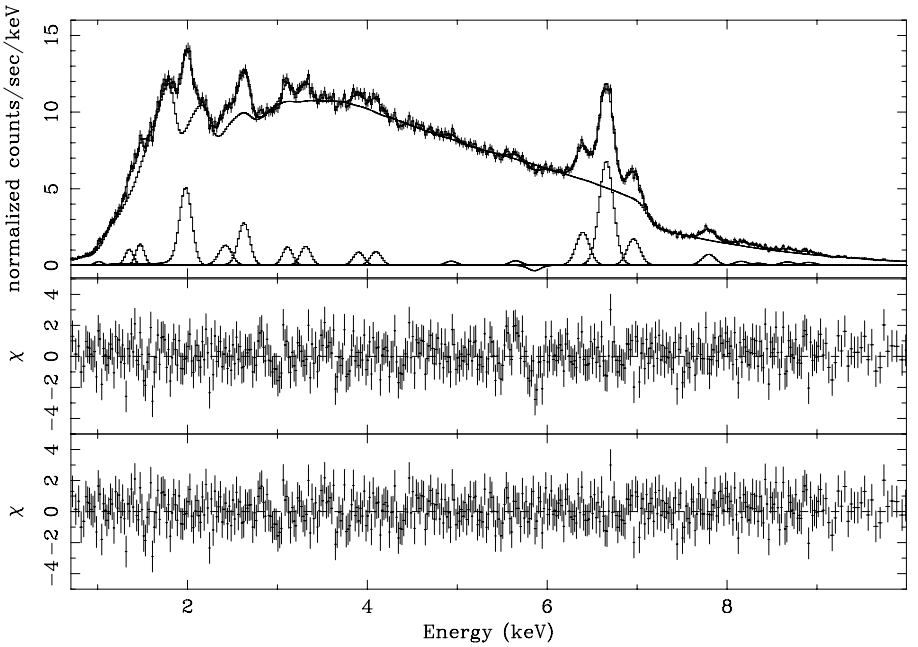

FIGURE 2. Top Panel: pn Spectrum of Cir X–1 in the 0.7–10 keV energy band (all the lines used to obtain the best fit are plotted). **Middle Panel:** Residuals after the addition of the identified absorption edges ans emission lines, a structure is evident between 5.5 and 6 keV. **Bottom Panel:** Residuals after the addition of an emission line at 5.6 keV and an absorption line at 5.85 keV.

blackbody temperature and normalization are 1.2 keV and 0.025, respectively. The equivalent hydrogen column associated to the interstellar matter is 1.2×10^{22} cm^{-2}, the equivalent hydrogen column associated to the neutral matter embedding the system is around 1×10^{24} cm^{-2}, the covered fraction of the emitting surface is 75%. We note a straordinary richness of absorption edges and emission lines in the residuals. Initially we add to the models the absorption edges keeping fixed the threshold energies (except that for Fe XXVI). We added the absorption edges associated to Si I, O VIII, Ne IX, Ne X, Si XIV, Ca I, Fe XXV, and Fe XXVI. The parameters of the continuum emission and the optical depths, τ, associated to the absorption edges are reported in Tab. 1. We find upper limits of the Ca I and Fe XXV optical depths, while a large value of τ associated to the Si I absorption edge indicating an overabundance of silicon.

As second step we add the emission lines to the model. Below 1.5 keV we note the presence of three lines associated to Ne X, Mg XI, and Mg XII, since the low statistics between 0.7 and 1.5 keV we keep fixed their centroids to the rest lab and the widths to 10 eV (the Mg XI centroid is fixed to the value of the resonance line). At the same way, since the low statistics above 7 keV, we keep fixed the widths of the emission lines identified between 7 and 10 keV. In this energy range we identify the Ni XXVII and Ni XXVIII emission lines, and the Fe XXVI Ly$_\beta$, Ly$_\gamma$, and Ly$_\delta$ emission lines. In the energy range between 2 and 7 keV the line parameters are left free, we identify the Si XIV, S XV,

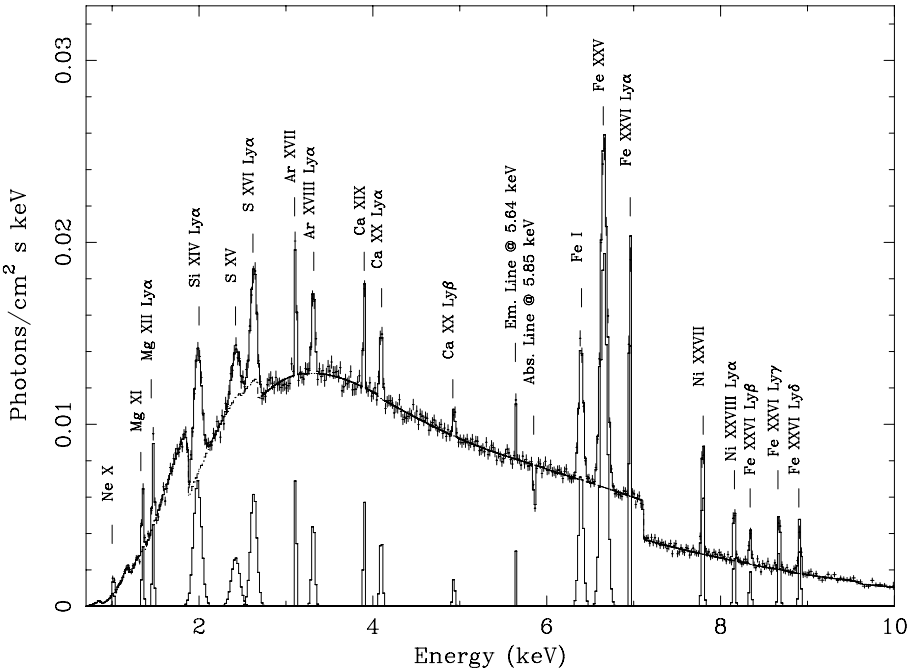

FIGURE 3. Unfolded spectrum of Cir X–1 corresponding to the best-fit model.

S XVI, Ar XVII, Ar XVIII, Ca XIX, Ca XX Ly$_\alpha$, Ca XX Ly$_\beta$, Fe I, Fe XXV, and Fe XXVI Ly$_\alpha$. In Fig. 2 (middle panel) we plot the residuals corresponding to the model composed of the continuum emission, absorption edges, and emission lines above reported. In Tab. 2 we report the parameters of the lines. Looking at the residuals a structure is evident between 5.5 and 6 keV. We fit this localized structure adding an emission and an absorption line at 5.6 and 5.85 keV, respectively, although we do not identify them. The emission and the absorption line are detected at 2.9σ and 3.9σ, respectively. In Fig. 2 (bottom panel) we plot the residuals after the adding of the lines between 5.5 and 6 keV, in Fig. 3 we plot the unfolded spectrum.

PRELIMINARY DISCUSSION

The 0.1–100 keV extrapolated absorbed and unabsorbed flux is 5.2×10^{-10} and 2.1×10^{-9} erg cm^{-2} s^{-1}, respectively. Adopting a distance to the source of 6.5 kpc (Stewart et al., 1993) the extrapolated 0.1–100 keV unabsorbed luminosity is 1×10^{37} erg s^{-1}. The corresponding blackbody radius is 6.2 ± 0.3 km.

The preliminary results of the fit indicate that near the zero phase (0.011–0.017) neutral matter embeds the source confirming the results of previous works (e. g. Brandt et al., 1996). Our work seems to suggest the simultaneous presence of ionized and neutral matter probably located in two different region around the system. Brandt &

Shulz (2000) and Shulz & Brandt (2002) detected the presence of P-Cygni profiles associated to highly ionized elements at similar phases, they assumed that the most plausible scenario producing these features was a wind moving along the radial direction above the accretion disc assuming the source almost edge-on. Looking at our results it is hard to sustain the edge-on scenario of Cir X–1 since in this case we cannot explain the presence of the prominent Fe I emission line, observed in the spectrum, requiring a lower inclination angle of the source. Our preliminary results seems to agree with the recent detection of a radio jet with angle separation between line of sight and jet direction of 5 degree (Fender et al., 2004) which implies a releasing of the edge-on scenario favoring a face-on one under the assumption that the radio-jet is directed almost perpendicularly to the equatorial plane. Finally we note another puzzling result, the continuum emission is well described using only a blackbody component. This result implies that we are observing only the emission from either the neutron star or the accretion disc because either one of the component is occulted or the accretion disc is not present. Both the scenarios are hard to be explained (assuming in the first case that the accretion disc is occulted) since it is natural to assume as mechanism producing the Fe I emission line the reflection from the disc. The remaining plausible scenario is the occulting of the neutron star but in this case it is anomalous the value of the inferred blackbody radius of 6 km. Finally we note the marginal detection of a structure between 5.5 and 6 keV modelled with an emission and an absorption line. The nature of this feature requires a more deep study that will be reported in a work in preparation.

REFERENCES

1. Begelman, M. C., McKee, C. F., Shields, G. A., 1983, ApJ, 271, 70
2. Brandt, W. N., & Schulz, N. S., 2000, ApJ, 544, L123
3. Fender R., Wu K., Johnston H. et al., 2004, Nature, 427, 222
4. Iaria, R.; Burderi, L., Di Salvo, et al., 2001a, ApJ, 547, 412
5. Iaria, R., Di Salvo, T., Burderi, L., Robba, N. R., 2001b, ApJ, 561, 321
6. Jansen, F., Lumb, D., Altieri, B., et al. 2001, A&A, 365, L1
7. Johnston, H. M., Fender, R., Wu, K., 1999, MNRAS, 308, 415
8. Murdin, P., Jauncey, D. L., Haynes, et al., 1980, A&A, 87, 292
9. Shulz, N. S., & Brandt, W. N., 2002, ApJ, 572, 971
10. Stewart, R. T., Caswell, J. L., Haynes, R. F., et al., 1993, MNRAS, 261, 593
11. Struder, L., Briel, U., Dennerl, K., et al. 2001, A&A, 365, L18
12. Tauris, T. M.; Fender, R. P.; van den Heuvel, E. P. J.; et al., 1999, MNRAS, 310, 1165
13. Tennant, A. F., Fabian, A. C., Shafer, R. A., 1986a, MNRAS, 219, 871
14. Tennant, A. F., Fabian, A. C., Shafer, R. A., 1986b, MNRAS, 221, 27P
15. Turner, M. J. L., Abbey, A., Arnaud, M., et al. 2001, A&A, 365, L27
16. Verner, D. A., Ferland, G. J., Korista, K. T., et al., 1996a, ApS, 465, 487
17. Verner, D. A., Verner, E. M., Ferland, G. J., 1996b, Atomic Data and Nuclear Data Tables, 64, 1